Microfabrication of Intelligent Biomimetic Networks for Recognition of D-Glucose

J. Zachary Hilt,[†,§] Mark E. Byrne,[†,⊥] and Nicholas A. Peppas*[,†,‡]

Biomaterials, Drug Delivery, Bionanotechnology and Molecular Recognition Laboratories, Department of Chemical Engineering, and Department of Biomedical Engineering, The University of Texas, University Code 0C400, Austin, Texas 78712-0231

Received June 8, 2006. Revised Manuscript Received September 19, 2006

Biomimetic, biocompatible polymer networks have been developed with tailored affinities, loading capacities, and transport properties for a given target molecule, and these networks promise to significantly impact a wide variety of biomedical fields, particularly diagnostic and therapeutic devices. Methods were developed to integrate these biomimetic networks with silicon substrates at the microscale, enabling the fabrication of microdevice platforms based on silicon technologies. Biomimetic polymer networks with recognition properties for D-glucose were micropatterned in fine dimensions onto silicon substrates and characterized by fluorescence and confocal microscopy studies. Novel copolymer networks containing poly(ethylene glycol)*n*dimethacrylate (where the number of EG repeat units $n = 1$, 4, and 14) at various cross-linking percentages (30, 67, and 80%) and acrylamide as a functional monomer were synthesized in polar, aprotic solvent with and without the target molecule present. Calculated diffusion constants for the target molecule decreased with decreasing cross-linker length, with the diffusion constant of PEG600DMA cross-linked networks being 5 times larger than that for the EGDMA-based networks. As the length of the cross-linking monomer increased, the target molecule affinity and capacity of the networks decreased. For networks demonstrating enhanced recognition, target molecule diffusion constants of control networks were approximately half of the recognitive network's value. Because diffusion was approximately Fickian, response times were extrapolated for thinner samples, which indicated the high potential for thin films of recognitive materials (i.e., 10 μm to 100 nm) to be used as robust micro- and nanosensor materials for various sensor platforms (e.g., micro- and nanocantilevers).

Introduction

Recent advances in the detection of disease and the delivery of therapeutic agents have been achieved by combination of intelligent material design with advances in micro- and nanotechnology. There has been considerable work in the preparation of micro- and nanostructured biomaterials for various applications, such as nanocarriers for controlled and targeted drug delivery, micro- and nanopatterned surface-modified medical systems and devices, and systems for biological recognition.[1−2]

Intelligent materials, specifically those based on polymer networks, have been the focus of recent research.[3−7] In particular, biomimetic polymeric networks capable of molecular recognition have been prepared by molecularly designing structures with functional groups that exhibit interactions between the building blocks of biocompatible networks and specific target molecules based on a fundamental analysis of biology and by stabilizing these interactions by the conformation of the three-dimensional structure.[6,7] Tailoring the macromolecular framework can lead to these structures having sufficient molecular flexibility to allow for diffusion of solvent and analyte (target molecule) within the network.

Synthetic networks that can be designed to recognize and bind biologically significant molecules are of great importance and influence a number of emerging technologies. These synthetic materials and hybrids can be used as unique robust sensing systems in point-of-care diagnostic devices or be incorporated into existing biomedical technologies. Thus, new micro- and nanodevices can be developed that can aid in the sensing and removal of undesirable biomolecules, often accompanied by controlled delivery of therapeutic agents, thus restoring physiological profiles of compounds in the body.

Biomimetic methods are now used to build biohybrid systems or synthetic biomimetic materials (i.e., mimicking

* Corresponding author. E-mail: peppas@che.utexas.edu. Phone: (512) 471-8227. Fax: (512) 471-6644.

† Biomaterials, Drug Delivery, Bionanotechnology and Molecular Recognition Laboratories, Department of Chemical Engineering, The University of Texas.

§ J.Z.H. is currently an Assistant Professor in the Department of Chemical and Materials Engineering at the University of Kentucky.

⊥ M.E.B. is currently an Assistant Professor in the Department of Chemical Engineering at Auburn University.

‡ Department of Biomedical Engineering, The University of Texas.

(1) Langer, R.; Peppas, N. A. *AIChE. J.* **2003**, *49*, 2990−3006.
(2) Peppas, N. A. *Adv. Drug Deliv. Rev.* **2004**, *56*, 1529−1531.
(3) Miyata, T.; Uragami, T.; Nakamae, K. *Adv. Drug Delivery Rev.* **2002**, *54*, 79−98.
(4) Peppas, N. A.; Hilt, J. Z.; Khademhosseini, A.; Langer, R. *Adv. Mater.* **2006**, *18*, 1345−1360.
(5) Peppas, N. A.; Hilt, J. Z. In *Handbook of BioMEMs and Biomedical Nanotechnology*; Bashir, R., Wereley, S., Eds.; Kluwer: Amsterdam, 2006; pp 117−132.
(6) Byrne, M. E.; Park, K.; Peppas, N. A. *Adv. Drug Delivery Rev.* **2002**, *54*, 149−161.
(7) Hilt, J. Z.; Byrne, M. E. *Adv. Drug Delivery Rev.* **2004**, *56*, 1599−1620.

10.1021/cm061343k CCC: $33.50
Published on Web 11/16/2006

biological recognition) for molecular sensing, drug delivery, drug targeting, and tissue engineering devices.[8−10] The synthesis and characterization of biomimetic gels and molecularly imprinted drug release and protein delivery systems is a significant focus of recent research.[6,7,11−14] Configurational biomimetic imprinting of a drug within an intelligent gel leads to novel biomaterials that not only recognize and load drug but also act therapeutically by locally or systemically releasing a suitable amount in a tunable way.

The design of a precise macromolecular chemical architecture that can recognize target molecules from an ensemble of similar molecules has a large number of potential applications. The main thrust of past research in this field was in separation processes (chromatography, membrane separations, capillary electrophoresis, solid-phase extraction), immunoassays and antibody mimics, biosensor recognition elements, and catalysis and artificial enzymes.[15−18] Typically, these materials are more robust in regards to pH and temperature changes than biological-based systems, which normally have narrow ranges of operation.

Biosensors utilize proteins and/or other biological compounds to selectively recognize and sense a specific target. The major limitations of these natural receptors are their high cost, potential antigenicity, and low stability. An alternative to these techniques is to use synthetic biomimetic networks that are designed to bind and respond to specific ligand molecules. Biomimetic polymer networks are advantageous because they can be tailored to bind any molecule with controlled selectivity and affinity, provided that certain interactions exist.

Here, we investigate the nanoscale dynamics of novel biomimetic polymer networks as entirely synthetic recognition elements exhibiting tailored recognitive properties and function. The networks are rendered biocompatible by tethering or incorporating significant amounts of poly(ethylene glycol), which is known to be biocompatible and limit protein adsorption. For integration of these polymer networks at the micro- and/or nanoscale, procedures have been developed to facilitate patterning precise features and achieving spatial control. In particular, these studies build on our previous work[19−22] on intelligent hydrogels for novel biosensor platforms. Biomimetic polymer networks can play a similar role in developing novel sensor platforms for a wide variety of biological entities.

Experimental Section

Acrylamide (Aam), 2,2-dimethoxy-2-phenyl acetophenone (DMPA), dimethylsulfoxide (DMSO), ethylene glycol dimethacrylate (EGDMA), γ-methacryloxypropyl trimethoxysilane (γ-MPS), and D-glucose, were purchased from Aldrich (Milwaukee, WI). Poly(ethylene glycol)*n*dimethacrylate (PEG*n*DMA) grades, with $n = 200$, 400, and 600 (indicating the average molecular weight of the PEG chain and corresponding to 4.5, 9, and 14 repeating units, respectively), were obtained from Polysciences, Inc. (Warrington, PA). Irgacure 184, 1-hydroxycyclohexyl phenyl ketone, was purchased from Ciba Specialty Chemicals (Tarrytown, NY). Fluorescent D-glucose analogue, 2-(*N*-(7-nitrobenz-2-oxa-1,3-diazol-4-yl)amino)-2-deoxy-glucose (2-NBDG), was purchased from Molecular Probes, Inc. All chemicals were of analytical grade.

Recognitive Network Synthesis. Novel copolymer networks of differing composition and percentage of cross-linking monomer were synthesized as thin films in an aprotic, polar solvent via UV free-radical polymerization in a nitrogen atmosphere. On the basis of a biomimetic approach to emulate a glucose-binding protein docking site, we selected monomers with appropriate functional groups by analyzing corresponding glucose-binding protein residues such as aspartate, glutamate, and asparagine.[23] In a typical experiment (e.g., PEG200DMA as cross-linking monomer), 15 mmol of Aam and 60, 30, or 10 mmol of PEG200DMA (e.g., 80, 67, or 30% moles of cross-linking monomer/moles all monomers, respectively) were allowed to complex with 3 mmol of D-glucose mixed with 6 mL of DMSO. After mixing and checking mutual solubilities, Irgacure 184 initiator was added in the amount of 1−2 wt %. Control polymers were made with exactly the same composition except D-glucose was not added.

After preparation, the solution was placed in a nitrogen atmosphere and nitrogen was bubbled for 30 min to remove oxygen, which is a free-radical scavenger and inhibits the free-radical polymerization. The monomer mixtures were pipetted between two clamped 6 in. by 6 in. glass plates with a Teflon spacer that was 790 μm thick. Next, the glass plate assembly was placed under a UV source (Dymax Ultraviolet Flood Cure System) and exposed to UV light with an intensity of 10.0−15.0 mW/cm^2 for 15 min to initiate the free-radical polymerization.

Polymers were placed in deionized water immediately after preparation, carefully separated from the slides, and then cut into various diameter discs using a cork borer. Discs were then placed in 50 mL centrifuge tubes and placed on a rotating mixer (25 rpm, Glas-Col, Terre Haute, IN) and resuspended within multiple 24 h wash steps to remove glucose and excess monomer as verified by spectroscopic analysis. The resulting discs were then dried in air at ambient conditions and placed in a vacuum oven ($T = 26$ °C, 28 mmHg vacuum) until a constant weight was obtained (<0.1 wt % difference). The discs were then stored in a desiccator until testing.

Analysis of Binding/Recognitive Characteristics. Binding/recognitive studies and release experiments were conducted to examine the relative rates of analyte recognition (uptake) and release

(8) El-Sayed, M. E. H.; Hoffman, A. S.; Stayton, P. S. *Expert Opin. Biol. Ther.* **2005**, *5*, 23−32.
(9) Byrne, M. E.; Henthorn, D. B.; Huang, Y.; Peppas, N. A. In *Biomimetic Materials and Design: Biointerfacial Strategies, Tissue Engineering and Targeted Drug Delivery*; Dillow, A. K., Lowman, A., Eds.; Dekker: New York, 2002; pp 443−470.
(10) Venkatesh, S.; Byrne, M. E.; Peppas, N. A.; Hilt, J. Z. *Expert Opin. Drug Delivery* **2005**, *2*, 1085−1096.
(11) Oral, E.; Peppas, N. A. *J. Biomed. Mater. Res.* **2004**, *68A*, 439−447.
(12) Alvarez-Lorenzo, C.; Concheiro, A. *J. Chromatogr., B* **2004**, *804*, 231−245.
(13) Spizzirri, U. G.; Peppas, N. A. *Chem. Mater.* **2005**, *17*, 6719−6727.
(14) Bergmann, N. M.; Lauten, E. H.; Peppas, N. A. *Drug Delivery Syst. Sci.* **2005**, *4*, 35−40.
(15) Takeuchi, T.; Haginaka, J. *J. Chromatogr., B* **1999**, *728*, 1−20.
(16) Piletsky, S. A.; Alcock, S.; Turner, A. P. F. *Trends Biotechnol.* **2001**, *19*, 9−12.
(17) Piletsky, S. A.; Panasyuk, T. L.; Piletskaya, E. V.; Nicholls, I. A.; Ulbricht, M. *J. Membr. Sci.* **1999**, *157*, 263−278.
(18) Schweitz, L.; Andersson, L. I.; Nilsson, S. *J. Chromatogr., A* **1998**, *817*, 5−13.
(19) Ward, J. H.; Bashir, R.; Peppas, N. A. *J. Biomed. Mater. Res.* **2001**, *56*, 351−360.
(20) Hilt, J. Z.; Gupta, A. K.; Bashir, R.; Peppas, N. A. *Biomed. Microdevices* **2003**, *5*, 177−184.
(21) Bashir, R.; Hilt, J. Z.; Gupta, A.; Elibol, O.; Peppas, N. A. *Appl. Phys. Lett.* **2002**, *81*, 3091−3093.
(22) Byrne, M. E.; Oral, E.; Hilt, J. Z.; Peppas, N. A. *Polym. Adv. Technol.* **2002**, *13*, 798−816.
(23) Li, T.; Lee, H.; Park, K. J. *Biomater. Sci., Polym. Ed.* **1998**, *9*, 327−344.

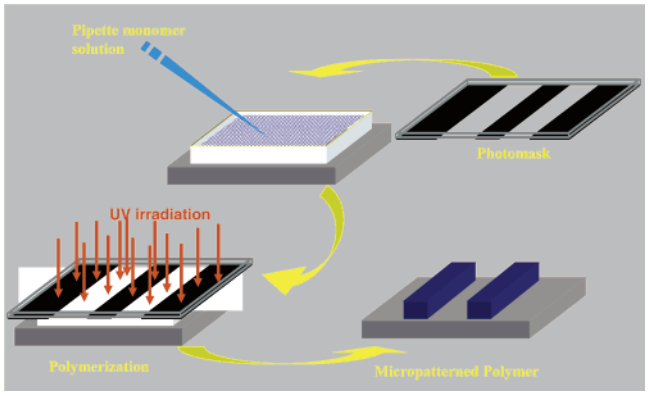

Figure 1. Schematic of the microreactor photolithography technique.

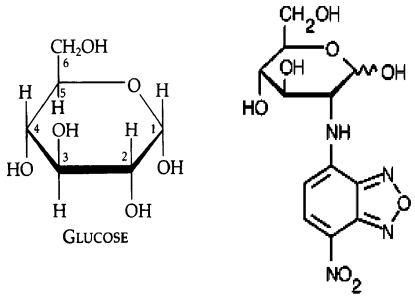

Figure 2. D-Glucose template and fluorescent analogue. In solution, glucose mutarotates between two conformations: the alpha (as shown, 30−35%) and beta (65−70%) positions of the carbon 1 hydroxyl group at equilibrium.

from the polymer networks. The effect of the network structure on the diffusion coefficient of the D-glucose fluorescent analogue, 2-NBDG (Figure 2, maximum absorption 466 nm; maximum emission 542 nm), was examined. The bound concentration of analyte was determined by analyzing fluorescence intensity values from polymer discs of equal thickness. In using fluorescence methods for quantitative analysis, it was critical to match all experimental parameters during analysis (objective and field of view, camera integration time, etc.), including excitation times, because fluorophore bleaching could alter intensity profiles.

To analyze the affinity of the recognitive polymer networks for glucose, we followed the binding of 2-NBDG in water using fluorescence microscopy. An aliquot of known concentration of 2-NBDG (1×10^{-4} mg/mL or 2.9×10^{-4} mM) was added to washed, solution-swollen polymer discs (preparation described previously) in 50 mL of DI water within centrifuge tubes. The tubes were covered with aluminum foil and placed on a rotating mixer (Glas-Col., Terre Haute, IN; 70°, 25 RPM). At various time points, kinetic analysis of the binding was carried out. Analysis of fluorescence intensity values from polymer discs of equal thickness provided quantitative analysis of binding.

A Nikon Eclipse ME600L fluorescence microscope with a FITC filter set was used and images were acquired with Coolsnap digital camera. Meta-View software from Universal Imaging was utilized to analyze a large number of pixels within these images for calculation of an average fluorescence intensity and standard deviation across the image.

Preparation of Recognitive Polymer Network Microstructures. A novel technique based on photolithography was utilized to pattern recognitive polymer networks onto silicon wafers. A schematic of the technique is included as Figure 1. This microreactor photolithography used a Teflon spacer with a thickness of approximately 12.5 μm to create the microreaction chamber. Silicon wafers were cleaved into pieces that were approximately 2 cm by 2 cm and then cleaned utilizing a standard Piranha clean. To promote covalent adhesion between the silicon surface and the polymer, the silicon pieces were soaked in a 10 wt % solution of γ-MPS in acetone for more than 2 h. The pieces were then rinsed in acetone followed by ethanol, and then air-dried. The organosilane coupling agent formed a self-assembled monolayer on the native silicon dioxide surface and presented methacrylate pendent groups that reacted and covalently bonded the silicon surface with the polymer film.

For these microscale studies, PEG200DMA was selected as the cross-linking agent for the recognitive networks with 67% cross-linking, because this system was demonstrated to exhibit substantial enhancement in the network affinity while allowing practical transport of the target molecule. Although networks cross-linked with EGDMA resulted in higher equilibrium binding, these systems exhibited a substantial reduction in target diffusion coefficient and thus the response time. For the micropatterning studies, monomer mixtures were prepared as described in the previous section.

The monomer mixture was pipetted onto the silicon pieces fitted with the Teflon spacer that had been cut to provide the desired reactor size. Next, polymer micropatterns were created by UV free-radical polymerization using a Karl Suss MJB3 UV400 mask aligner, enabling pattern alignment accuracies of 0.1 μm. After being brought into contact with the mask, the microreactor assembly was exposed to UV light with an intensity of 11.0 mW/cm^2 or 23.0 mW/cm^2 for exposure times of 30 s to 1 min. The pieces were then removed and allowed to soak in deionized, distilled water for more than 24 h to remove any unreacted monomer and template. As before, the control polymer networks were prepared under identical conditions except for the absence of D-glucose.

For side-by-side patterning, the control network was patterned onto the silicon substrate first, and the sample was then washed to remove any unreacted monomer. The monomer solution containing the template molecule was then applied to the substrate, again using the microreactor assembly. Afterward, a Karl Suss MJB3 UV400 mask aligner was utilized for control over the spatial positioning of the micropatterns. Finally, the sample was brought in contact with the mask and exposed to UV light, with equivalent intensities as previously described. The pieces were then removed and allowed to soak in deionized, distilled water for more than 24 h to remove any unreacted monomer and the template.

Recognitive Polymer Network Microstructure Characterization. The binding results of the polymer micropatterns were visualized using the fluorescent glucose analogue 2-NBDG. 2-NBDG was added at a concentration of 4.7×10^{-7} mol/L to 50 mL centrifuge tubes containing the samples with the polymer micropatterns and allowed to equilibrate via rotating mixing before fluorescence imaging, as described previously. By analyzing fluorescence intensity values from polymer patterns of equal thickness, we can determine a quantitative analysis of the amount of 2-NBDG bound in the network.

In addition, confocal microscopy analysis was performed using a Bio-Rad MRC 1024 Confocal Microscope with an MRC 1024 system. Images, z-sections, etc., were collected using LaserSharp software, and image analysis was conducted using Confocal Assistant software. Confocal fluorescence imaging permitted fluorescence emission from a single optical plane, and a combination of all optical planes yielded a three-dimensional image.

Results and Discussion

Uniform and isotropic films of recognitive polymer networks were successfully prepared via UV free-radical polymerization. The relative affinities of these networks for the target molecule, D-glucose, were analyzed. The time-dependent response of these systems were analyzed, because

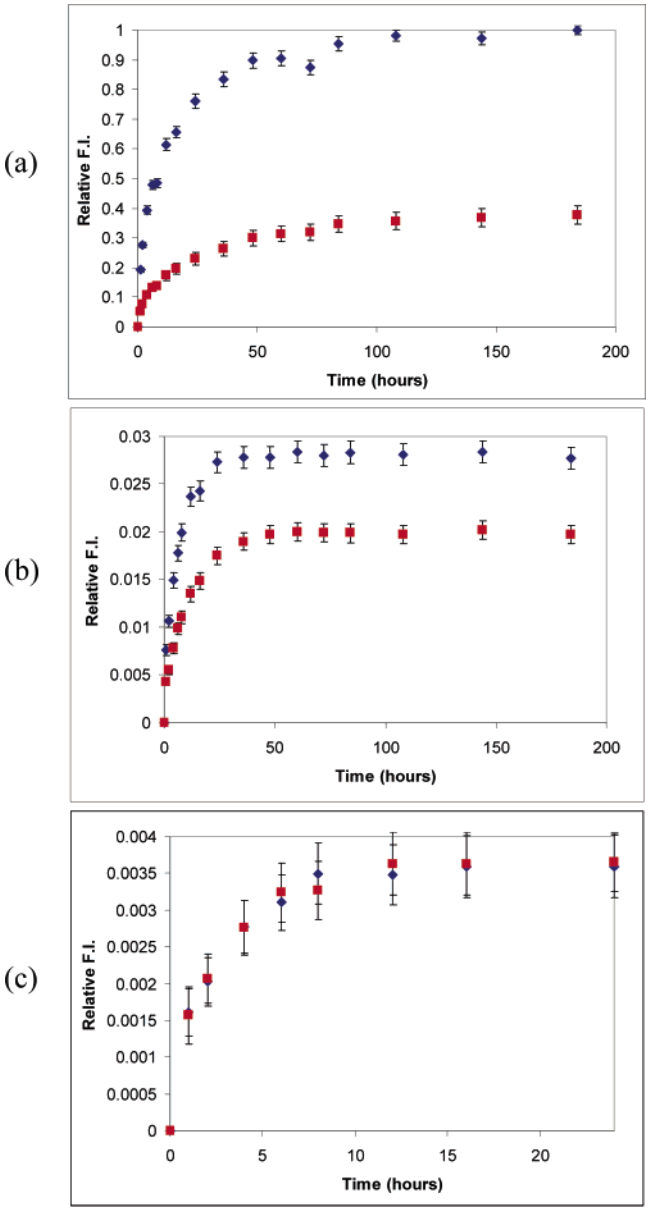

Figure 3. Kinetic binding results for recognitive (blue diamonds) and control (red squares) poly(acrylamide-co-PEGnDMA)-based copolymers with (a) 67% EGDMA cross-linking percentage, (b) 67% PEG200DMA cross-linking, and (c) 67% PEG600DMA cross-linking (relative fluorescence intensity, F.I., is reported as the fluorescence intensity divided by the maximum fluorescence intensity of the 67% EGDMA recognitive system). ($N = 3 \pm$ SD).

potential sensing applications require analysis and understanding of the response time, which is the time necessary to reach the ligand recognition/binding equilibrium.

The time-dependent binding results for the target analyte are presented for recognitive and control acrylamide-based polymer systems with 67 mol % cross-linking agent with varying average molecular weight of PEG (recognitive data with polymer networks cross-linked with EGDMA in Figure 3a, with PEG200DMA in Figure 3b, and with PEG600DMA in Figure 3c). It is observed that, as the molecular weight of the PEG cross-linker is increased, the time to reach equilibrium binding is decreased. Therefore, the gels with a higher molecular weight of the cross-linking monomers result in looser networks, which allow for faster diffusion of the target analyte. This was also consistently observed for the systems with 30 and 80% cross-linking percentages. Selectivity studies were carried out on bulk networks, and selectivity was determined by the ratio of the equilibrium association constants between D-glucose and D-galactose. For poly(Aam-co-PEG200DMA) networks with a 67% cross-linking percentage, the selectivity was 1.6.

Also, as the average molecular weight of the cross-linking monomer increased, the affinity, capacity, and selectivity of the network for the ligand decreased. This is due to the increased molecular mobility and increased mesh size within the polymer network as the average molecular weight of the cross-linking monomer increases.

To determine whether a transport process is diffusion controlled, early time data can be fit to the following empirical relationship[24]

$$\frac{M_t}{M_\infty} = kt^n \tag{1}$$

where M_t is the total cumulative mass of penetrant absorbed (or released) at time t, M_∞ is the total cumulative mass of penetrant absorbed (or released) at equilibrium, and k and n are characteristic constants of the penetrant−polymer system. For slab geometry, as is used in these studies, an n value of 0.5 indicates Fickian diffusion, a value between 0.5 and 1 indicates anomalous diffusion, and a value of 1 indicates case II transport.

The Fickian diffusion equation for one-dimensional solvent transport may be solved for the slab geometry used in these studies. For geometries with aspect ratios (diameter/thickness) greater than 10, it has been shown that edge effects can be ignored and that the problem can be approached as a one-dimensional process governed by Fick's second law, resulting in the following solution[25]

$$\frac{M_t}{M_\infty} = 1 - \frac{8}{\pi^2}\sum_{n=0}^{\infty}\frac{1}{(2n+1)^2}\exp\left(-\frac{D(2n+1)^2\pi^2 t}{\delta^2}\right) \tag{2}$$

At short times ($0 < M_t/M_\infty < 0.6$), eq 2 can be written as

$$\frac{M_t}{M_\infty} \cong 4\left(\frac{Dt}{\pi\delta^2}\right)^{1/2} \tag{3}$$

This can be written in terms of the weight swelling ratio, q

$$\frac{M_t}{M_\infty} = \frac{q-1}{q_\infty - 1} \tag{4}$$

For the acrylamide-based polymer systems cross-linked with 67% PEG200DMA, the power law fit and early time fit for Fickian diffusion in a slab geometry were applied to determine the power law exponent, n, and the diffusion coefficient of 2-NBDG in these polymer networks; these values are included in Table 1. All systems exhibited n values of approximately 0.5, and solute transport can therefore be described by Fickian diffusion. The calculated 2-NBDG diffusion coefficients decreased with decreasing cross-linker

(24) Ritger, P. L.; Peppas, N. A. *J. Controled Release* **1987**, *5*, 23−26.
(25) Crank, J. *The Mathematics of Diffusion*; Oxford University Press: Oxford, U.K., 1975.

Table 1. 2-NBDG Diffusion Coefficients and Power Law Exponents Recognitive and Control Polymer Networks with Varying Cross-Linker Length

cross-linking %	cross-linker	recognitive (R) or control (C)	2-NBDG diffusion coefficient ($\times 10^7$ cm^2/s)	power law exponent
67	EGDMA	R	1.06	0.46
		C	0.53	0.46
67	PEG200DMA	R	2.25	0.46
		C	1.27	0.46
67	PEG600DMA	R	5.37	0.39
		C	5.48	0.41

Table 2. Response Times (approximate time to 90% equilibrium) for the Imprinted Polymer Networks with Varying Cross-Linker Length and Feed Percentage (δ is the thickness of the film)

cross-linking %	cross-linker	response time (h) $\delta = 790\ \mu$m	response time (s) $\delta = 10\ \mu$m	response time (s) $\delta = 100$ nm
30	EGDMA	6	3.5	3.5×10^{-4}
30	PEG200DMA	4	2.3	2.3×10^{-4}
30	PEG600DMA	2	1.2	1.2×10^{-4}
67	EGDMA	60	35	3.5×10^{-3}
67	PEG200DMA	24	14	1.4×10^{-3}
67	PEG600DMA	8	4.6	4.6×10^{-4}

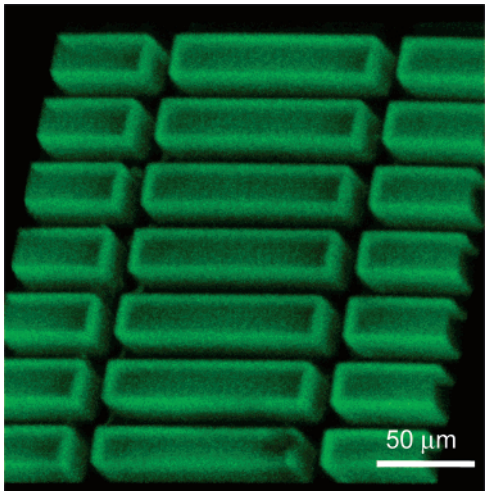

Figure 4. Three-dimensional projection of micropatterned rectangular array of a biomimetic recognitive polymer network with 67% PEG200DMA cross-linking obtained utilizing a confocal microscope.

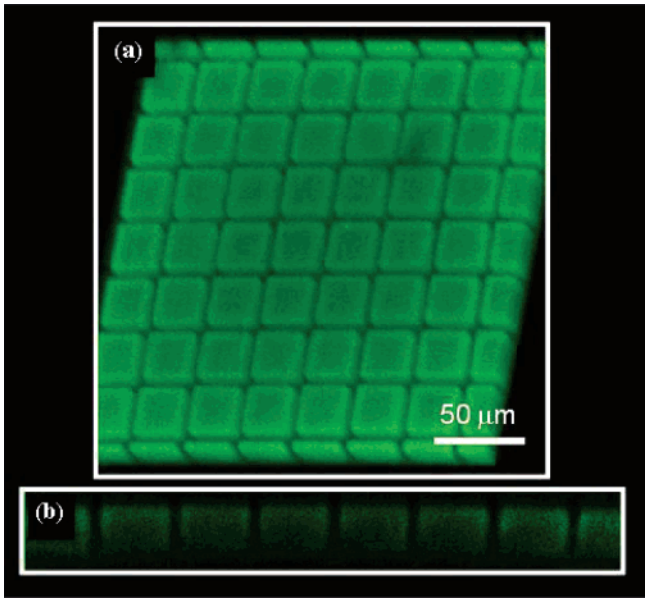

Figure 5. (a) Three-dimensional projection of a micropatterned square array of a biomimetic polymer network with 67% PEG200DMA cross-linking obtained utilizing a confocal microscope. (b) Slice of the square array.

length, with the 2-NBDG diffusion coefficients of acrylamide-based networks cross-linked with PEG600DMA being 5 times larger than for the same network cross-linked with EGDMA.

Analysis of 2-NBDG diffusion through recognitive networks cross-linked with EGDMA or PEG200DMA indicated that the 2-NBDG diffusion coefficient through the neat (nonimprinted) networks was approximately one-half the value of the diffusion coefficient for the recognitive (imprinted) networks. This enhancement of the diffusion coefficients in the imprinted networks was caused by the increased nanoscale porosity resulting from polymerization in the presence of a template molecule, which acts as a porogen. This is in agreement with previous studies examining the effect of template molecules on polymerizations.[26−28] However, this effect was not observed for the recognitive networks prepared with the highest-molecular-weight cross-linking agent (PEG600DMA).

In Table 2, the response time, i.e., the time required to achieve 90% of the equilibrium recognitive value, is reported for the bulk samples (thickness of 790 μm). Because the kinetic response was described by Fickian, the response times were extrapolated for thinner samples, which correspond to size ranges for which they will be applied in microdevices. It is important to emphasize the value of these polymer networks as synthetic sensor elements, especially when applied as micro- and nanostructures.

Using the microreactor photolithography technique, we created micropatterns of recognitive polymer networks on silicon substrates. Representative 3D projection images of micropatterned recognitive polymer networks are shown in Figures 4 and 5. The thickness of the patterned polymer films was determined to be approximately 13 μm using profilometry. The confocal microscopy images illustrate the precise patterns that can be created on silicon substrates using these methods. It also indicated that binding was not only on the surface of the polymer gels but homogeneously distributed throughout the matrix. Although all rectangle and square patterns in these figures are imprinted for D-glucose, this demonstration is significant. The techniques utilized here can be extended for preparing micro- or nanoscale arrays with

(26) Ward, J. H.; Peppas, N. A. *J. Controlled Release* **2001**, *71*, 183−192.
(27) Ward, J. H.; Furman, K.; Peppas, N. A. *J. Appl. Polym. Sci.* **2003**, *89*, 3506−3519.
(28) Oral, E.; Peppas, N. A. *Polymer* **2004**, *45*, 6163−6173.

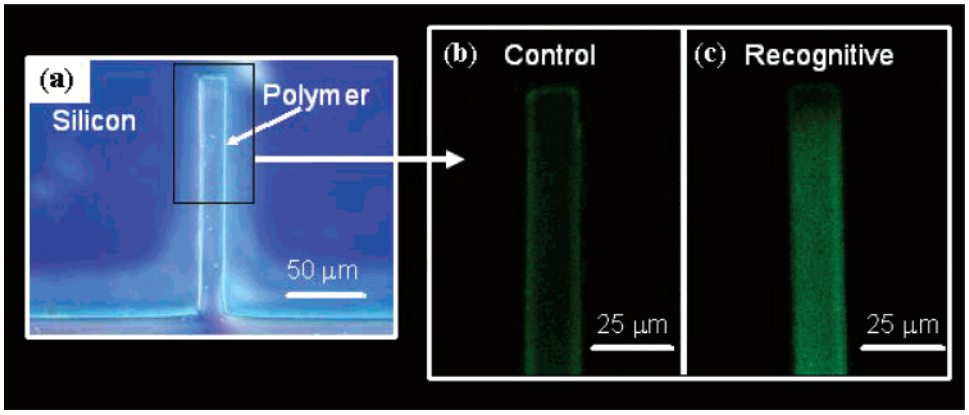

Figure 6. (a) Nomarski image of a biomimetic polymer network with 67% PEG200DMA cross-linking patterned in the shape of a cantilever. (b,c) Confocal microscope slice through the middle of a cantilever pattern of a (b) control and (c) biomimetic recognitive network.

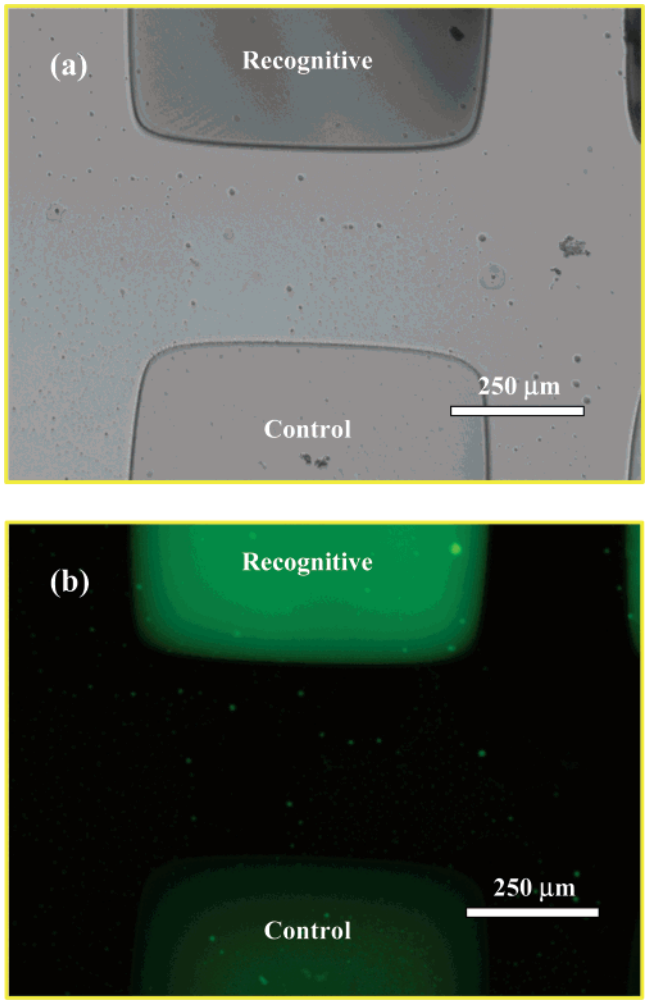

Figure 7. (a) Bright-field and (b) fluorescent image of a biomimetic and control polymer network with 67% PEG200DMA cross-linking patterned side-by-side. Again, the biomimetic network demonstrates a higher fluorescence intensity due to a higher affinity for the fluorescent analogue, 2-NBDG.

hundreds or thousands of different recognitive polymer networks, allowing for large-scale robust assays to be developed.

In Figure 6, microcantilever patterns of a control polymer network and a recognitive polymer network are qualitatively compared. In Figure 6a, a brightfield image illustrates the precise polymer structures that can be created at the microscale. In panels b and c of Figure 6, confocal microscopy z-slices at approximately 5 μm below the surface of the patterns are shown. Comparing panels b and c of Figure 6, it is evident that the recognitive polymer network has bound more of the fluorescent analogue. These results illustrate the potential power of applying these polymer systems for microarray and microsensing applications, such as microcantilever-based systems.

In Figure 7, bright-field and fluorescent images of recognitive polymer networks and control networks patterned side-by-side are presented, enabling simultaneous imaging and analysis within a single microscope field of view. A mask aligner was utilized to enable precise side-by-side micropatterning of ultrathin polymers films via UV free-radical polymerization; this is particularly advantageous for quantitative analysis, where experimental parameters have to be precisely matched for comparison to be made. As expected, the time required to reach equilibrium binding and recognition was less than a minute because of the decrease in the size of the structure. The corresponding fluorescent image (Figure 7b) of the recognitive and control polymer networks patterned side-by-side demonstrated a bound ratio (recognitive template bound over control) of 2.2. This value is in accordance with previous observations of binding behavior (i.e., the same binding concentration yielded an equivalent value for bulk polymers, and Figure 3b demonstrates a 2-NBDG bound ratio of 1.5). These results indicate that side-by-side florescence intensity analysis in the same field of view can also be accomplished with separate samples by careful experimental analysis.

Conclusions

Novel recognitive polymer networks were developed that are entirely synthetic and tailored to have various properties and functions. In this study, biomimetic polymer networks designed to recognize D-glucose via noncovalent complexation were micropatterned in fine dimensions. Micropatterning results qualitatively and quantitatively demonstrate that these recognitive macromolecular networks have tailored affinity and capacity for the target molecule, D-glucose and can be effectively micropatterned in a number of relevant configurations without a loss of function due to diffusional restrictions. These results are encouraging and will guide the application of these materials as functional components of

micro- and nanoscale biosensors and diagnostic devices, because the techniques are applicable to other biologically significant molecules and biomimetic polymer networks, in which hydrogen bonding, hydrophobic, or ionic contributions will direct recognition.

Recent developments in the field of micro- and nanoscale therapeutics and diagnostics could not have been predicted 20 years ago. Likewise, robust, biocompatible, biomimetic recognition systems as presented in this paper show great promise in future devices that will extend from a laboratory setting and be placed at the point of care in a disposable fashion.

Acknowledgment. The work presented here was supported by grants from the National Science Foundation (BES-9706538) and the National Institutes of Health (GM56231, GM43337, EB 000246). M.E.B. and J.Z.H. were also NSF IGERT Fellows (Grant DGE-99-72770) during a portion of this work.

CM061343K